



Continuous freeze-drying of messenger RNA lipid nanoparticles enables storage at higher temperatures

Sofie Meulewaeter^{a,b}, Gust Nuytten^c, Miffy H.Y. Cheng^d, Stefaan C. De Smedt^{a,b},
Pieter R. Cullis^d, Thomas De Beer^c, Ine Lentacker^{a,b,*}, Rein Verbeke^{a,b,*}

^a Laboratory of General Biochemistry and Physical Pharmacy, Faculty of Pharmaceutical Sciences, Ghent University, Ghent 9000, Belgium.

^b Cancer Research Institute Ghent (CRIG), Ghent University Hospital, Ghent University, Ghent 9000, Belgium

^c Laboratory of Pharmaceutical Process Analytical Technology, Faculty of Pharmaceutical Sciences, Ghent University, Ghent 9000, Belgium

^d Department of Biochemistry and Molecular Biology, University of British Columbia, Vancouver, British Columbia V6T 1Z3, Canada

ARTICLE INFO

Keywords:

mRNA lipid nanoparticle
Vaccine
Lyophilization
Stability
Continuous freeze-drying
Cryo-EM

ABSTRACT

Messenger RNA (mRNA) lipid nanoparticles (LNPs) have emerged at the forefront during the COVID-19 vaccination campaign. Despite their tremendous success, mRNA vaccines currently require storage at deep freeze temperatures which complicates their storage and distribution, and ultimately leads to lower accessibility to low- and middle-income countries. To elaborate on this challenge, we investigated freeze-drying as a method to enable storage of mRNA LNPs at room- and even higher temperatures. More specifically, we explored a novel continuous freeze-drying technique based on spin-freezing, which has several advantages compared to classical batch freeze-drying including a much shorter drying time and improved process and product quality controlling. Here, we give insight into the variables that play a role during freeze-drying by evaluating the impact of the buffer and mRNA LNP formulation (ionizable lipid to mRNA weight ratio) on properties such as size, morphology and mRNA encapsulation. We found that a sufficiently high ionizable lipid to mRNA weight ratio was necessary to prevent leakage of mRNA during freeze-drying and that phosphate and Tris, but not PBS, were appropriate buffers for lyophilization of mRNA LNPs. We also studied the stability of optimally lyophilized mRNA LNPs at 4 °C, 22 °C, and 37 °C and found that transfection properties of lyophilized mRNA LNPs were maintained during at least 12 weeks. To our knowledge, this is the first study that demonstrates that optimally lyophilized mRNA LNPs can be safely stored at higher temperatures for months without losing their transfection properties.

1. Introduction

During the coronavirus disease 2019 (COVID-19) pandemic, messenger RNA (mRNA) vaccines have emerged at the forefront. Less than one year after the pandemic outbreak, two mRNA vaccines were granted conditional marketing authorization for the prevention of COVID-19 as a first-of-its-kind vaccine technology, i.e. BNT162b2 (Comirnaty®) and mRNA-1273 (Spikevax®) developed by Pfizer/BioNTech and Moderna, respectively [1]. These vaccines both consist of N1-methylpseudouridine (m1ψ)-modified mRNA encoding the viral spike antigen, encapsulated in a lipid nanoparticle (LNP) which is composed of a proprietary ionizable cationic lipid, 1,2-distearoyl-sn-glycero-3-phosphocholine (DSPC), cholesterol, and a polyethylene glycol (PEGylated) lipid [2,3].

Despite their tremendous success in the COVID-19 pandemic, a drawback of mRNA vaccines is their poor stability, which consequently requires cold chain storage at low or even ultra-low temperatures [4,5]. To exemplify, Moderna's Spikevax® vaccine and bivalent booster have a shelf-life of 9 months when kept at −50 °C to −15 °C and can only be stored for 30 days at refrigerator temperatures after thawing [6]. The formulation consists of mRNA LNPs suspended in Tris (20 mM) buffer containing 8.7 m/V% sucrose as cryoprotectant [7]. Comirnaty® even requires storage at −90 °C to −60 °C, preserving its stability for 12 months [8]. For its pediatric formulation and bivalent booster, Pfizer switched the buffer from phosphate-buffered saline (PBS) containing 10% sucrose to Tris (10 mM) 10% sucrose [9], which suggests that the buffer composition is important for the stability of mRNA LNPs. Indeed, due to this adaptation, the shelf-life at refrigerator temperatures could

* Corresponding authors.

E-mail addresses: Ine.Lentacker@UGent.be (I. Lentacker), Rein.Verbeke@UGent.be (R. Verbeke).

¹ Last authors contributed equally to this work.

be increased from 1 month to 10 weeks while long-term storage at $-60\text{ }^{\circ}\text{C}$ to $-90\text{ }^{\circ}\text{C}$ is guaranteed for up to 12 months [10,11].

In comparison, other types of marketed COVID-19 vaccines can be stored at refrigerator temperatures, ranging from 6 months in the case of Vaxzevria® (an adenovirus vector vaccine by AstraZeneca/Oxford) [12], to 9 months for Nuvaxovid® (a protein-based vaccine by Novavax) [13], up to even 11 months for Jcovden® (an adenovirus vector vaccine by Janssen) [14]. Notwithstanding the ability of these vaccines to be stored at higher temperatures than mRNA vaccines, they still require cold chain logistics which demand well-trained personnel to maximally prevent the wastage of inadequately stored vaccines [15]. However, when vaccines need deep freeze storage, such as the current mRNA vaccines, cold chain logistics become even more challenging as this demands specialized infrastructure including expensive ultracold freezers [16]. For these reasons, vaccines requiring (deep freeze) cold chain logistics not only demand extensive organization but also become less accessible for low- and middle-income countries [15].

A potential solution to improve the shelf-life of mRNA LNP vaccines at higher temperatures is to develop a lyophilized formulation. Lyophilization or freeze-drying is a method to eliminate water from a heat-labile formulation. In a dehydrated state, hydrolysis is less likely to take place while also molecular mobility is drastically reduced, slowing down degradation reactions [17]. Lyophilization comprises a freezing phase and a drying phase, both of which are known to induce stresses to lipid-based nanoparticle formulations [18–20]. Therefore, lyoprotectants are typically added to protect liposomal and RNA LNP formulations during freeze-drying [19,20]. Two theories have been proposed to explain the working mechanism of lyoprotectants, namely the water replacement theory and the vitrification theory. The water replacement theory states that sugars can interact with phospholipids (in case of e.g. liposomes) via hydrogen bonds, so as to replace water molecules during freeze-drying and conserve the structure of the lipid membrane [18]. On the other hand, the vitrification theory proposes that sugars can freeze-concentrate and subsequently undergo vitrification to form a glass matrix with high viscosity, preventing changes in lipid membranes [18]. Recently, a few reports were published that investigated the role of lyoprotectants during freeze-drying of RNA LNPs [21–23]; some other studies showed that mRNA LNPs could be successfully lyophilized and stored without really digging into a mechanistic understanding [24,25]. Although these prior studies have demonstrated the feasibility of lyophilization of RNA LNPs, a thorough investigation of the factors that could play a role in freeze-drying of RNA LNPs has not yet been discussed. For instance, as freezing rate, ionic strength, and changes in pH are frequently reported to impact the outcome of lyophilization, they should also be considered when optimizing a lyophilization process for mRNA LNPs [19].

In previous studies on this topic, batch freeze-drying of RNA LNPs was performed [26]. It should be noted, however, that such batch processes have some drawbacks, including a long (and expensive) process and drying time, mostly ranging from 1 to 7 days [27]. Furthermore, vial-to-vial variability is inherent to the process and can lead to altered critical quality attributes (CQAs) of the individual vials [28]. Also, it is not possible to perform any in-process controls of individual vials [28]. Finally, scaling batch freeze-drying processes from lab-scale to pilot-scale to production-scale is very time-consuming as well. Because of these limitations and the general incentive toward continuous manufacturing by regulatory authorities [29], a continuous process for the freeze-drying of RNA LNPs was evaluated in this study. More specifically, we explored spin-freezing and radiative drying, as developed by Corver et al. [30] In this method, vials are spun along their longitudinal axis during the freezing step, causing the fluid to spread over the lateral surface of the glass vial. As a consequence, a frozen product is obtained with a larger surface area allowing a faster heat- and mass transfer and thus shortened drying time [28]. Subsequently, during the drying phase, the vials move along a series of infrared (IR)-heaters in a low-pressure environment. In contrast to batch freeze drying, this

technology results in a drastic reduction of drying time, improved process control, and 100% product quality control [28].

Here, we present a method to lyophilize mRNA LNPs by continuous freeze-drying based on spin-freezing. The nucleoside-modified mRNA LNPs comprised the ionizable lipidoid C12–200 but resembled the COVID-19 mRNA vaccines with respect to helper lipids and lipid molar ratios. First, we evaluated the effect of buffer type (PBS, phosphate, and Tris at different buffer capacities) and lipid:mRNA weight (wt) ratio on the lyophilization of mRNA LNP formulations. To this end, we compared lyophilized mRNA LNPs to freshly prepared control mRNA LNPs in terms of size, polydispersity (PDI), zeta potential, encapsulation efficiency, and transfection efficiency. We demonstrated that a sufficiently high lipid:mRNA wt ratio and an optimal buffer (phosphate or Tris) were necessary to prevent leakage of encapsulated mRNA, and thus to maintain the functionality of the mRNA LNPs. We then studied the stability of optimally lyophilized mRNA LNPs stored at various temperatures ($4\text{ }^{\circ}\text{C}$, $22\text{ }^{\circ}\text{C}$, and $37\text{ }^{\circ}\text{C}$) for a period of 12 weeks. When stored at higher temperatures, compared to non-lyophilized mRNA LNPs, the stability of lyophilized mRNA LNPs was drastically improved. Finally, we validated the functionality of lyophilized mRNA LNPs in vivo, by measuring luciferase expression of fresh and lyophilized firefly luciferase (fLuc) encoding mRNA LNPs. We believe that this study provides important insights into lyophilization of mRNA LNPs and reveals potential for the storage of mRNA LNPs at higher temperatures, which may ease the logistics and transportation of these novel vaccines.

2. Materials and methods

2.1. *In vitro* transcription of mRNA

Enhanced green fluorescent protein (eGFP)- and firefly luciferase (fLuc)-encoding mRNA were synthesized by *in vitro* transcription (IVT) from pGEM4Z-GFP-64A and pBlue-Luc-A50 respectively. The plasmids were purified using a QIAquick PCR purification kit (Qiagen, Venlo, The Netherlands) and linearized using the *Spe* I or *Dra* I restriction enzymes (Promega, Leiden, The Netherlands) for the pGEM and the pBlue plasmid respectively. IVT was performed starting from the linearized pDNA by using the T7 MegaScript kit (ThermoFisher Scientific), including an Anti-Reverse Cap Analog (Jena Bioscience, Germany) and chemically modified N1-methylpseudouridine-5'-triphosphate (Jena Bioscience, Germany) instead of uridine. After being digested with DNase I, IVT mRNA was precipitated with LiCl and washed with 70% ethanol. The absorbance at 260 nm was measured to calculate the concentration. IVT mRNA was stored at $-80\text{ }^{\circ}\text{C}$ at a concentration of $1\text{ }\mu\text{g}/\mu\text{l}$ until used.

2.2. mRNA LNP production

LNPs were formulated by rapid mixing of an aqueous phase containing mRNA dissolved in a 25 mM sodium acetate buffer at pH 4 and an ethanol phase containing lipids dissolved at a total concentration of 10 mM. Lipids comprised the ionizable lipidoid C12–200 (Corden Pharma, Plankstadt, Germany) and helper lipids distearoylphosphatidylcholine (DSPC), Cholesterol and 1,2-dimyristoyl-rac-glycero-3-methoxypropyl-ethylene glycol-2000 (DMG-PEG2000) (Avanti Polar Lipids, Birmingham, AL, USA) at 50/10/38.5/1.5 mol% respectively. The two phases were prepared at an aqueous:ethanol volume ratio of 3:1, and mRNA and lipids were combined at a C12–200:mRNA weight ratio of either 10:1 or 20:1, while the lipid composition (molar ratios of the lipids) was maintained in both formulations. Both phases were loaded into a syringe (BD) and inserted in the NxGen microfluidic cartridge for mixing using a NanoAssemblr Ignite instrument (Precision Nanosystems). Microfluidic mixing was performed at a total flow rate (TFR) of 12 ml/min and a flow rate ratio (FRR) of 3:1 RNA:lipid. The waste volumes were 0.25 ml and 0.05 ml at the start and the end respectively. The resulting mRNA LNP suspension was then

divided over different dialysis cassettes (Pur-A-Lyzer™ Maxi Dialysis Kit 0.1–3 mL, MWCO, 12–14 kDa, Merck) and dialyzed for 5 h at 4 °C against Tris (Fisher Scientific), Phosphate (Merck) or PBS-buffer (ThermoFisher Scientific) at 20 or 40 mM (Tris) or 10 or 20 mM (PBS and phosphate) at pH 7.4. For stability studies, mRNA LNPs in aqueous solution were stored in temperature-controlled rooms at 4 °C and 22 °C.

2.3. Freezing and freeze-drying of mRNA LNPs

For both freezing and freeze-drying of mRNA LNPs, equal volumes of mRNA LNPs and protectant (25 m/V% sucrose or trehalose (Merck) dissolved in Tris-, Phosphate- or PBS-buffer at pH 7.4) were mixed to yield an LNP suspension with a final concentration of 15.6 µg/ml mRNA and 12.5 m/V% lyoprotectant. When mRNA LNPs were stored frozen, aliquots containing the aqueous solutions were transferred to a –20 °C freezer. In the case of freeze-drying, type I glass vials (2 ml) (Schott, Müllheim, Germany) were filled with 400 µl of the protectant solution and 400 µl of mRNA LNP suspension containing 12.5 µg of mRNA. The LNP formulation was freeze-dried using spin freeze-drying, which is the basis for a continuous freeze-drying technology that has extensively been described in literature [31–35]. Vials were inserted into a WB6000-D overhead stirrer (Wiggins, Beijing, China) using a custom-made 2 ml vial adapter and subsequently rotated along their longitudinal axis at 4000 rpm resulting in a thin liquid layer spread over the inner vial wall. The rotating vial was then exposed to compressed air that was cooled using a liquid nitrogen heat exchanger to a temperature of around –60 °C. The gas flow rate was controlled using a Bronkhorst F-202AV mass flow controller (Flowcor, Olen, Belgium) and set to a constant rate of 18 l/min or 80 l/min, which resulted in a slow or fast freezing rate, respectively. Vial temperature was measured using a FLIR A655sc thermal camera (Thermal Focus, Ravels, Belgium), and vials were frozen and cooled to a final temperature of –50 °C. Then, the vials were semi-stoppered and dried under a vacuum using conductive heat transfer. After drying, the vials were backfilled with nitrogen gas to atmospheric pressure and stoppered before retrieval and capping. To evaluate stability during the freeze-drying process, lyophilized vials were reconstituted using 400 µl of Tris-, Phosphate- or PBS-buffer at pH 7.4 immediately after the cycle was finished. To evaluate stability during storage, lyophilized vials were transferred to temperature-controlled rooms at 4 °C, 22 °C, and 37 °C and reconstituted at set timepoints.

2.4. Characterization of mRNA LNPs

LNPs were diluted to 0.6 ng/µl mRNA in HEPES 20 mM at pH 7.4 and transferred into a folded capillary zeta cell (DTS1070) to measure size and PDI by Dynamic Light Scattering (DLS) using the Zetasizer Nano ZS (Malvern Panalytical). A refractive index (RI) of 1.45 and absorption of 0.001 was set for the material, while an RI of 1.330 and viscosity of 0.8872 cP were used for the dispersant. Samples were equilibrated to 25 °C and measurements were made with 10 s run durations with the number of runs automatically determined. Each measurement had a fixed position of 5.5 mm in the cuvette with an automatic attenuation selection. Diameters are reported as number-average. Zeta potential was measured by Electrophoretic Light Scattering (ELS) using the same device and settings as described above.

The encapsulation efficiency of mRNA LNPs was quantified using the Quant-iT RiboGreen Assay (Life Technologies). Samples were diluted in TE buffer and 1% Triton TE buffer in such a way that a concentration of about 0.1 µg/ml of total mRNA was reached in the final sample, after which diluted samples were incubated for 10 min at 37 °C. The assay was performed according to the manufacturer's protocol in a black 96-well plate, using a calibration curve with and without Triton. The plate was analyzed with Victor 3 fluorescent plate reader (Perkin-Elmer) using an excitation of 485 nm and emission of 535 nm. The background fluorescence was subtracted from each sample. The encapsulation efficiency was determined by comparing the signal of the RNA-binding

fluorescent dye RiboGreen™ in the absence (free mRNA) and presence (total mRNA) of Triton.

2.5. Cell culture and transfection

HEK293T cells were maintained in DMEM medium (Biowest) supplemented with 10% fetal bovine serum (Biowest) and 1% penicillin/streptomycin/L-glutamin (Gibco-Invitrogen) and incubated at 37 °C, 5% CO₂. Twenty-four hours before transfection, cells were seeded in 24-well plates at a density of 150 × 10³ cells per well in 500 µl cell culture medium. Transfections were performed in triplicate and a fixed volume of 16 µl corresponding with a theoretical amount of 0.5 µg eGFP mRNA-loaded LNPs was added to each well to transfect the cells. After 24 h, cells were stained to identify dead cells using a 7-AAD live/dead stain (ThermoFisher) and were analyzed using the MACSQuant 16 flow cytometer (Miltenyi Biotec) to quantify eGFP-expression.

2.6. Cryo-electron microscopy

mRNA LNPs were dialyzed against PBS or Tris and subsequently lyophilized in presence of 12.5 m/V% sucrose. Before vitrification, mRNA LNPs were reconstituted and concentrated using Amicon centrifugal filter units (Millipore) to reach a concentration of 10–25 mg/ml of total lipid. In order to create vitreous ice, mRNA LNPs were applied to glow-discharged copper grids (3–5 µl), and plunge-frozen with an FEI Mark IV Vitrobot (FEI, Hillsboro, OR). Grids were placed into the microscope after being transferred into a Gatan 70° cryo-tilt transfer system that had been pre-equilibrated to at least –180 °C. All samples were imaged using an FEI Eagle 4 K CCD camera on an FEI LaB6 G2 TEM (FEI, Hillsboro, OR) running at 200 kV under low-dose conditions. To improve contrast, all samples were scanned at 55,000 x magnification with a nominal under-focus of 1–2 µm. The UBC Bioimaging Facility handled all sample preparation and imaging (Vancouver, BC).

2.7. In vivo fLuc expression in mice

Female C57BL/6 mice (6 weeks old) were purchased from Envigo (Gannat, France) and housed in an SPF facility. All animal experiments were conducted according to the regulations of Belgian law and approved by the local Ethical Committee. Mice received 3 µg fLuc mRNA in a total volume of 50 µl via intramuscular (i.m.) injection in the hind leg muscle. Five hours after the injection, mice were anesthetized in a ventilated anesthesia chamber with 3% isoflurane in oxygen and the thigh was depilated with hair removal cream. Subsequently, VivoGlo Luciferin (Promega) was administered intraperitoneally (i.p.). After 10 min, bioluminescence images (BLI) were acquired by the IVISlumina II system (PerkinElmer, Waltham, MA, USA). Quantitative analysis of the images was performed using the LivingImage software (PerkinElmer).

2.8. Statistical analysis

All data are presented as mean ± standard deviation. All statistical analyses were performed using the GraphPad software Prism 8 (La Jolla, CA, USA). Information on the analysis is specified in the figure captions.

3. Results

3.1. Ionizable lipid-to-mRNA ratio and formulation buffer play a crucial role in the freeze-drying of mRNA LNPs

The first set of experiments was designed to find a suitable formulation that resists the stresses to which the mRNA LNPs are exposed during lyophilization. To this end, we evaluated two main variables: the ionizable lipid:mRNA wt ratio and the buffer. The LNPs were prepared via microfluidic mixing using the NanoAssemblr Ignite system and were based on the formulation reported by Leuschner et al. [36] and were

composed of the ionizable lipidoid C12–200 and the helper lipids DSPC, cholesterol, and DMG-PEG 2000 at molar ratios of 50:10:38.5:1.5 mol% respectively. The mRNA encoded eGFP and was nucleoside-modified using m1Ψ instead of normal uridine. Hence, this formulation was similar to mRNA LNPs in Comirnaty® and Spikevax® as m1Ψ-modified mRNA and the same molar ratio of lipids were used. However, the ionizable lipid used in mRNA vaccines listed above were based on ALC-0315 and SM-102 respectively [37], while we made use of C12–200.

As illustrated in Fig. 1, mRNA LNPs were formulated at a C12–200:mRNA wt ratio of either 10 or 20 (with the same lipid molar ratios) to study to which extent a higher amount of lipids in LNPs contributed to the stability of the mRNA LNP formulation during freeze-drying. Furthermore, the buffers which are used in the marketed mRNA vaccine formulations (PBS and Tris with a pH of 7.4) were evaluated at respectively a high and low buffer capacity and were supplemented with 12.5 m/V% sucrose as lyoprotectant. Finally, we also tested phosphate as a third buffer since we aimed to investigate the effect of the presence of the salt components during lyophilization [20].

After freeze-drying and reconstitution in the corresponding buffer, we assessed the properties of lyophilized mRNA LNPs by measuring size (reported as number mean), PdI, zeta potential, and mRNA encapsulation efficiency. For all formulations, the size and PdI did not significantly increase after lyophilization (Fig. 2A & B). However, we observed a drastic decrease in encapsulation efficiency and amount of mRNA encapsulated in the LNPs after lyophilization of mRNA LNPs formulated at a C12–200:mRNA wt ratio of 10. This was most pronounced for mRNA LNPs dialyzed in PBS with a lowering of the encapsulation efficiency from 85% to only 58% (Fig. 2C). Also, the zeta potential of the mRNA LNPs turned more negative (Fig. 2E). Increasing the buffer capacity could not prevent leakage of encapsulated mRNA and decline of the zeta potential. However, and importantly, at a C12–200:mRNA wt ratio of 20, the encapsulation efficiency of the lyophilized mRNA LNPs was only

lowered when PBS was used (92% to 72%), whereas the properties of mRNA LNPs dispersed in phosphate- and Tris buffer did not change upon lyophilization (Fig. 2D & F).

Next, we compared the transfection efficiency of the lyophilized formulations with their non-lyophilized counterparts in HEK293T cells (Fig. 2G & H). In Tris and phosphate buffer, mRNA LNPs preserved their transfection efficiency at the high C12–200:mRNA wt ratio, irrespective of the buffer capacity. As expected from the loss in mRNA encapsulation, transfection efficiency decreased drastically ($\pm 30\%$) when the mRNA LNPs were dispersed in PBS. At low C12–200:mRNA ratio, we observed a decreased transfection efficiency for PBS at both buffer capacities tested, while for phosphate and Tris the transfection efficiency was slightly reduced at high and low buffer capacity, respectively.

Taken together, our data indicate that the C12–200 mRNA LNPs could be successfully lyophilized in a formulation containing 12.5 m/V% sucrose, when the C12–200:mRNA wt ratio was increased from 10 to 20, and when PBS was replaced by Tris or phosphate buffer. Additionally, we also evaluated if we could improve the outcome of lyophilization of LNPs with a C12–200:mRNA wt ratio of 10 suspended in Tris 20 mM. To this end, we varied the freezing rate (slow and fast) and lyoprotectant (12.5 m/V% sucrose and trehalose) as this is typically done to optimize freeze-drying protocols [19]. We observed that a fast freezing rate was superior. However, although we could slightly improve the freeze-drying process when trehalose was used as a lyoprotectant, we were not able to fully prevent the negative effects of lyophilization on transfection efficiency, encapsulation efficiency, and zeta potential (supplementary fig. S1).

3.2. Formulation buffer affects morphology of mRNA LNPs upon formation and lyophilization

To gain more insight into the behavior of mRNA LNPs during

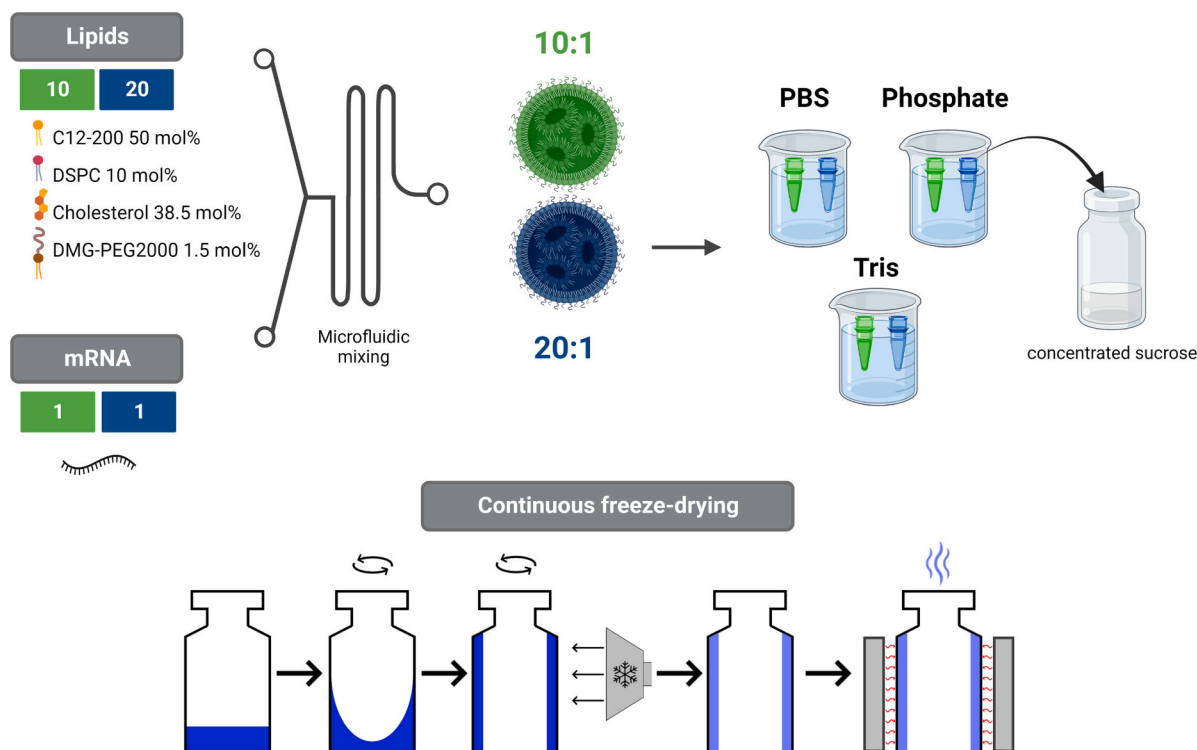


Fig. 1. Illustration of lyophilization procedure. mRNA LNPs were formulated at a C12–200:mRNA wt ratio of 10 or 20, by rapidly mixing the lipids (dissolved in ethanol) with mRNA in an acidic aqueous buffer (pH 4) using the microfluidic-based Nanoassemblr® Ignite system. The resulting dispersions were then dialyzed using either PBS, phosphate- or Tris-buffer at a low (10, 10 or 20 mM respectively) or a high (20, 20 or 40 mM) buffer capacity at pH 7.4. Next, the buffer was supplemented with 12.5 m/V% sucrose as lyoprotectant and vials were lyophilized by continuous freeze-drying based on spin-freezing. Figure is created with [bio-render.com](#)

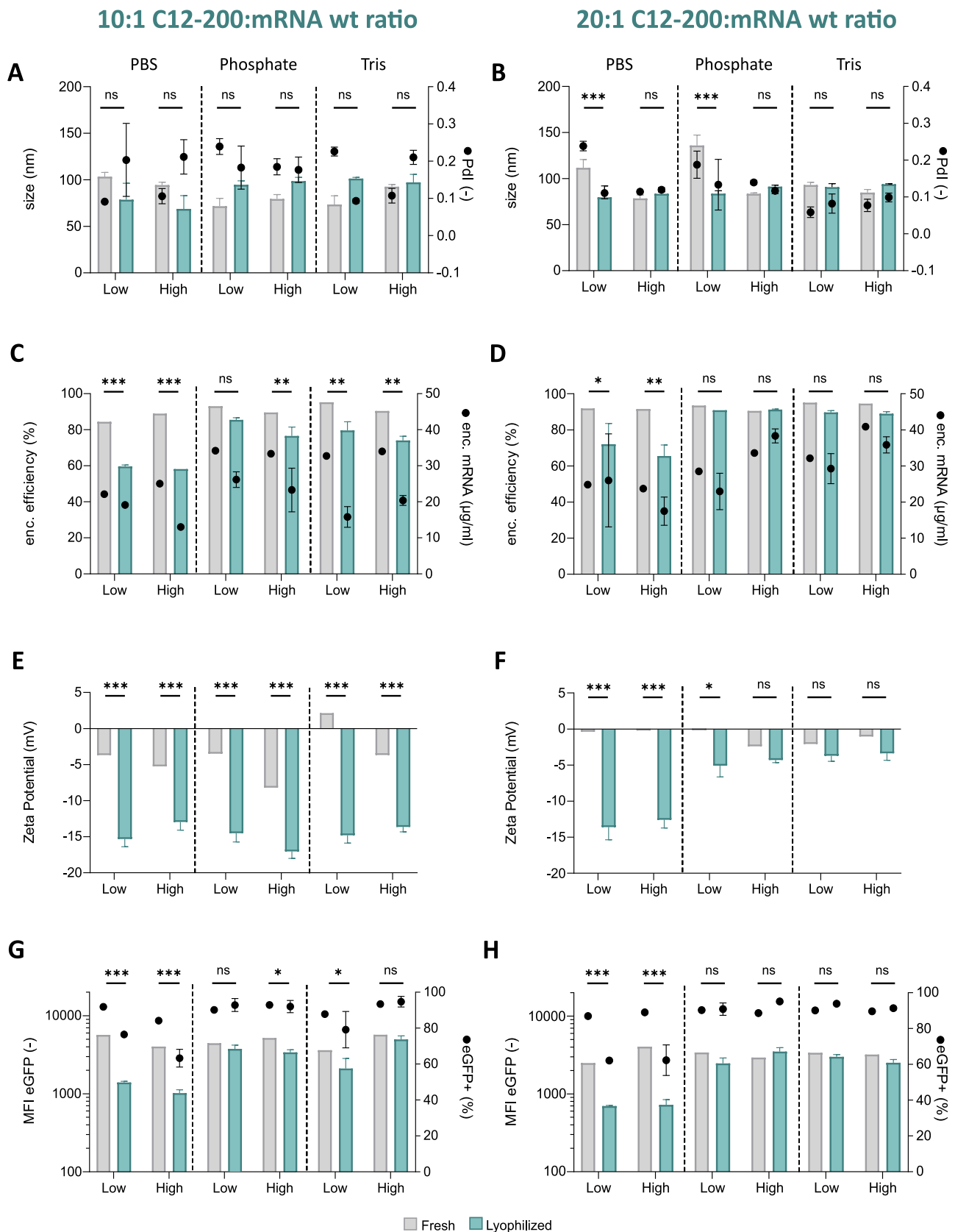


Fig. 2. Characteristics of mRNA LNPs (C12–200:mRNA wt ratio 10 and 20) before and after lyophilization in different buffers with low and high buffer capacity. Measurements were performed before and after lyophilization. (A, B) Size and PDI(●) determined via DLS. (C, D) Encapsulation efficiency and amount of encapsulated mRNA (●) determined via RiboGreen assay. (E, F) Zeta Potential of mRNA LNPs measured via ELS. (G, H) Transfection efficiency in HEK293T cells expressed as MFI eGFP in viable cells and eGFP+ cells (●). Mean values are shown. Error bars represent standard deviation ($n = 3$ lyophilized vials). Multiple unpaired t -test was performed with Holm-Sidak correction * p % 0.05, ** p % 0.01, *** p % 0.001.

lyophilization, cryo-electron microscopy (cryo-EM) was performed to identify the morphology of mRNA LNPs before and after freeze-drying. More specifically, we evaluated the morphology of mRNA LNPs with a C12–200:mRNA wt ratio of 20 suspended in either Tris or PBS, as these buffers showed to have a different impact on the stability of mRNA LNPs during lyophilization. Simultaneously, mRNA LNPs were evaluated for their size (DLS), zeta potential, encapsulation efficiency and transfection efficiency (supplementary fig. S2).

Cryo-EM unveiled that both the dialysis buffer and the freeze-drying process influenced the morphology of mRNA LNPs (Fig. 3). mRNA LNPs that were dialyzed in Tris consisted of a solid amorphous core, as previously described for mRNA/siRNA LNPs [38–40]. Interestingly, dialysis in PBS resulted in mRNA LNPs showing heterogenous morphology, including LNPs containing aqueous compartments (so-called ‘blebs’) which appeared to contain mRNA [40]. Moreover, some of these blebs completely dissociated from the LNP and formed liposomal structures. The different morphologies also responded differently to the lyophilization process. Some of the LNPs suspended in Tris formed blebs upon lyophilization, most likely as a result of phase separation induced by physical stress, as previously reported [40,41]. In contrast, lyophilization of mRNA LNPs suspended in PBS yielded multilamellar structures, which were mostly absent of the aqueous pockets observed in the fresh LNPs in PBS.

3.3. Lyophilization of mRNA LNPs in Tris buffer enhances their stability at higher temperatures

First, we studied the stability of mRNA LNPs stored in the fridge

(4 °C) for a period of 12 weeks. Based on the results shown in Fig. 2, we formulated mRNA LNPs at a C12–200:mRNA wt ratio of 20 in Tris or phosphate buffer with a pH of 7.4 at a low buffer capacity (Tris 20 mM and phosphate 10 mM) was chosen and 12.5 m/V% sucrose was added as a lyoprotectant. Physicochemical characteristics and transfection efficiency of mRNA LNPs were measured at the start (fresh, week 0) and at specified time points (after 7 days, 9 weeks and 12 weeks of storage) and are shown in Fig. 4.

Transfection of HEK293T cells (Fig. 4A & B) showed at multiple time points that mRNA LNPs in Tris buffer maintained their transfection efficiency during the study period, both in aqueous and lyophilized conditions. In contrast, the transfection efficiency of lyophilized mRNA LNPs diminished after only 1 week of storage in case phosphate was used as a buffer. In Fig. 4C & D, a drop in encapsulation efficiency was observed in LNPs stored in Tris buffer in aqueous condition which was not observed in lyophilized samples. The encapsulation efficiency in lyophilized phosphate-buffered mRNA LNPs at the end of the study was 3–4% higher compared to the start (Fig. 4C), this could be caused by small variations of the RiboGreen assay, which was previously seen in other stability studies [23,25]. Finally, the size did not significantly increase during the study period in all tested conditions (Fig. 4E & F). Additionally, we also studied the stability at –20 °C and found that mRNA LNPs can be stored at –20 °C when using the same buffers as those used for lyophilization in previous experiments. The LNPs preserved their transfection efficiency, encapsulation efficiency, and size in both Tris- and phosphate buffer (supplementary fig. S3).

Although mRNA LNPs were stable for 12 weeks at 4 °C, it should be noted that this still requires cold chain logistics. For this reason, we also

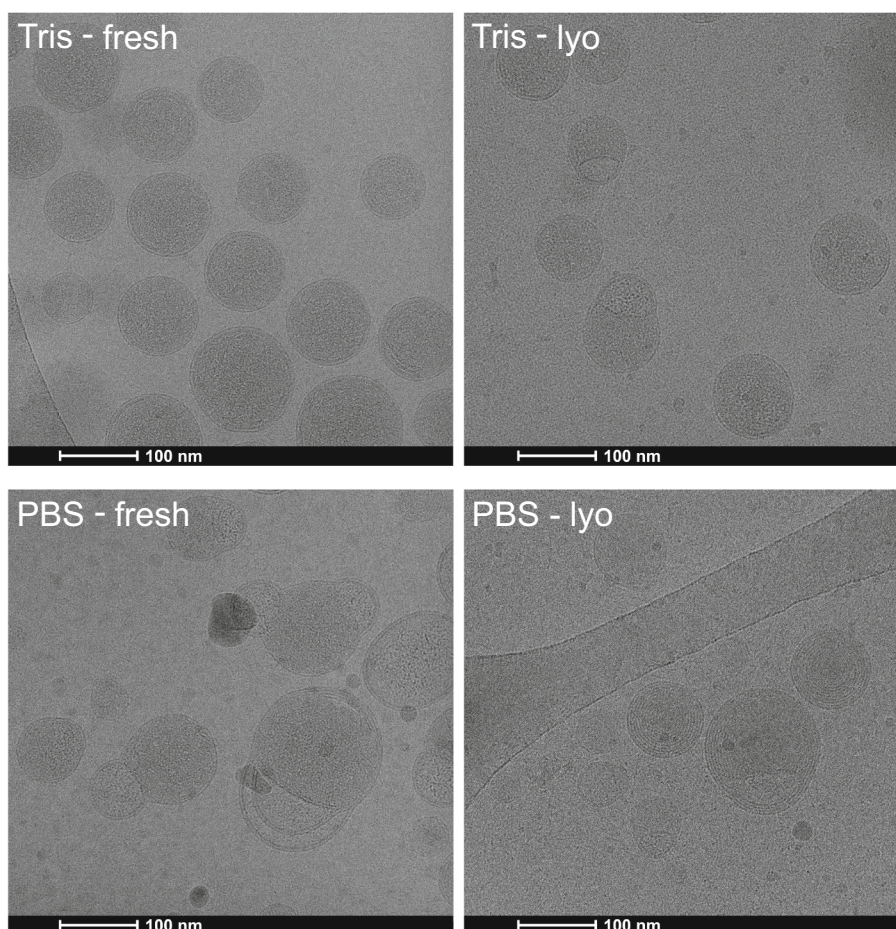


Fig. 3. Morphology of mRNA LNPs upon dialysis and lyophilization in Tris or PBS. Representative cryo-EM images of mRNA LNPs (C12–200:mRNA wt ratio 20) before and after lyophilization in Tris 20 mM and PBS 10 mM. Scale bars represent 100 nm.

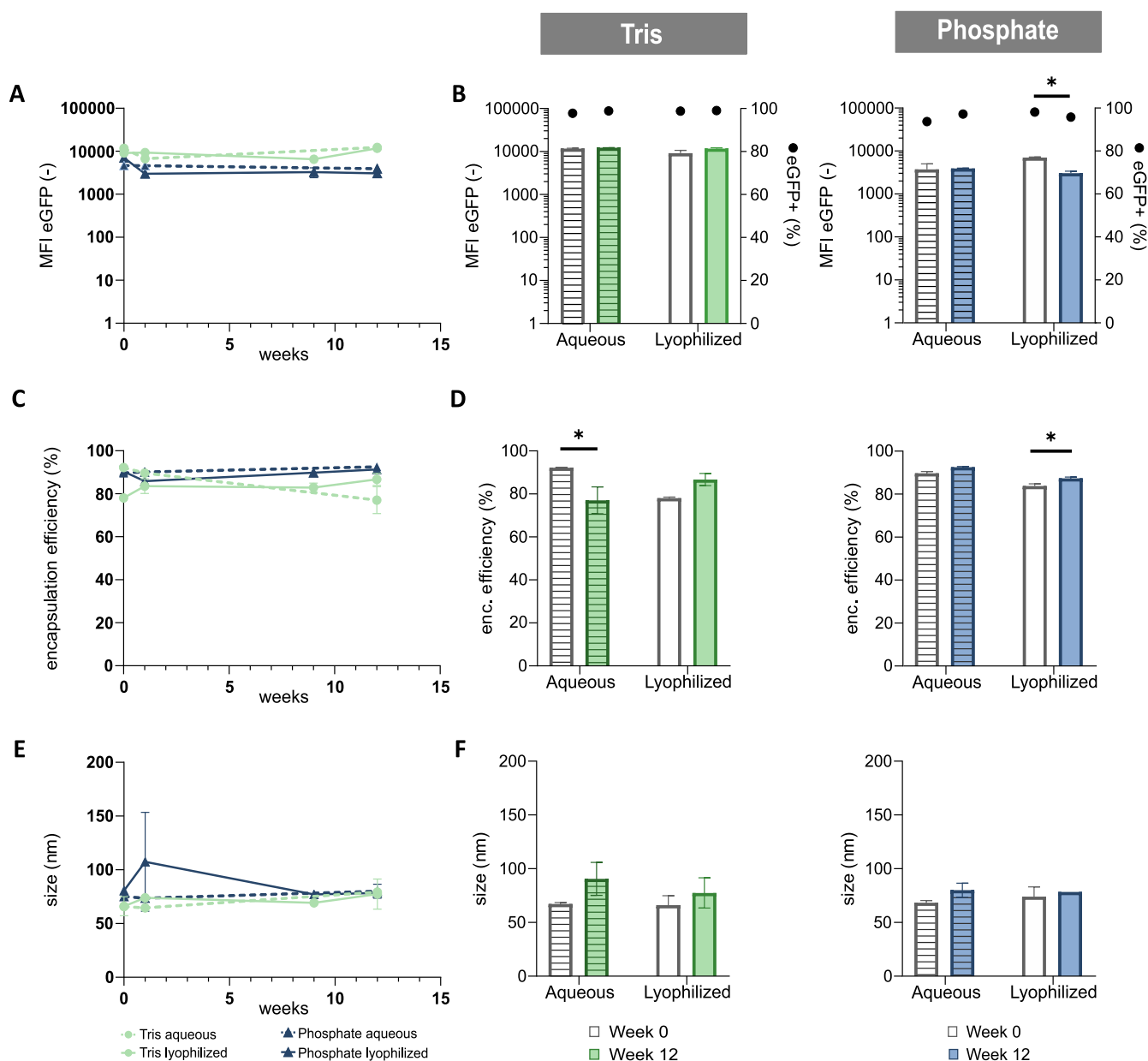


Fig. 4. Stability of aqueous and lyophilized mRNA LNPs at 4 °C. eGFP encoding mRNA LNPs were formulated at a C12–200:mRNA wt ratio of 20 and subsequently dialyzed in Tris 20 mM or phosphate 10 mM with a pH of 7.4. mRNA LNPs were either stored as an aqueous dispersion (dashed lines and bars) or lyophilized powder in the presence of 12.5 m/V% sucrose (full line) at 4 °C. (A, B) Transfection efficiency in HEK293T cells expressed as MFI eGFP in viable cells shown as a function of time (A) and at w0 and w12 only (B). (C, D) Encapsulation efficiency determined via RiboGreen assay shown as a function of time (C) and at w0 and w12 only (D). (E, F) Size determined via DLS shown as a function of time (E) and at w0 and w12 only (F). Mean values are shown. Error bars represent geometric SD ($n = 2$ vials). One-way ANOVA was performed using Holm-Sidak correction. * $p < 0.05$, ** $p < 0.01$, *** $p < 0.001$.

investigated if lyophilization could enhance stability of mRNA LNPs stored at room temperature (RT, 22 °C) or at even higher temperatures (37 °C). mRNA LNPs were formulated at a C12–200:mRNA wt ratio of 20 (in Tris 20 mM; pH 7.4) using 12.5% sucrose as lyoprotectant; stability was monitored for 12 weeks. Thus mRNA LNPs were stored respectively in aqueous condition at 22 °C and in lyophilized condition at 22 °C and 37 °C. Results are shown in Fig. 5.

For the aqueous mRNA LNP dispersions stored at room temperature (RT, 22 °C) we observed a drastic decrease in both the number of transfected cells and the MFI (reduction of 30% and 40% respectively) (Fig. 5A & B). In contrast, lyophilized samples did not lose their transfection efficiency after 12 weeks when stored at 22 °C or even at 37 °C, demonstrating the clear advantage of lyophilization. However, we noted an increase in particle size from 80 to 150 nm upon storage of

lyophilized mRNA LNPs at 37 °C (Fig. 5E & F). Furthermore, we also observed that storage at 22 °C and 37 °C slightly reduced the encapsulation efficiency of mRNA LNPs in aqueous and lyophilized conditions (Fig. 5C & D). It should however be noted that the encapsulation efficiency was maintained for 8 weeks, both for lyophilized and aqueous mRNA LNPs.

3.4. In vivo expression of mRNA LNPs is conserved after lyophilization

A previously reported study on lyophilized mRNA LNPs showed good preservation of transfection properties in vitro, but a loss of expression in vivo in mice upon lyophilization [21]. Therefore, we aimed to validate the functionality of the lyophilized mRNA LNPs after i.m. administration in mice. fLuc-encoding mRNA LNPs with a C12–200:mRNA

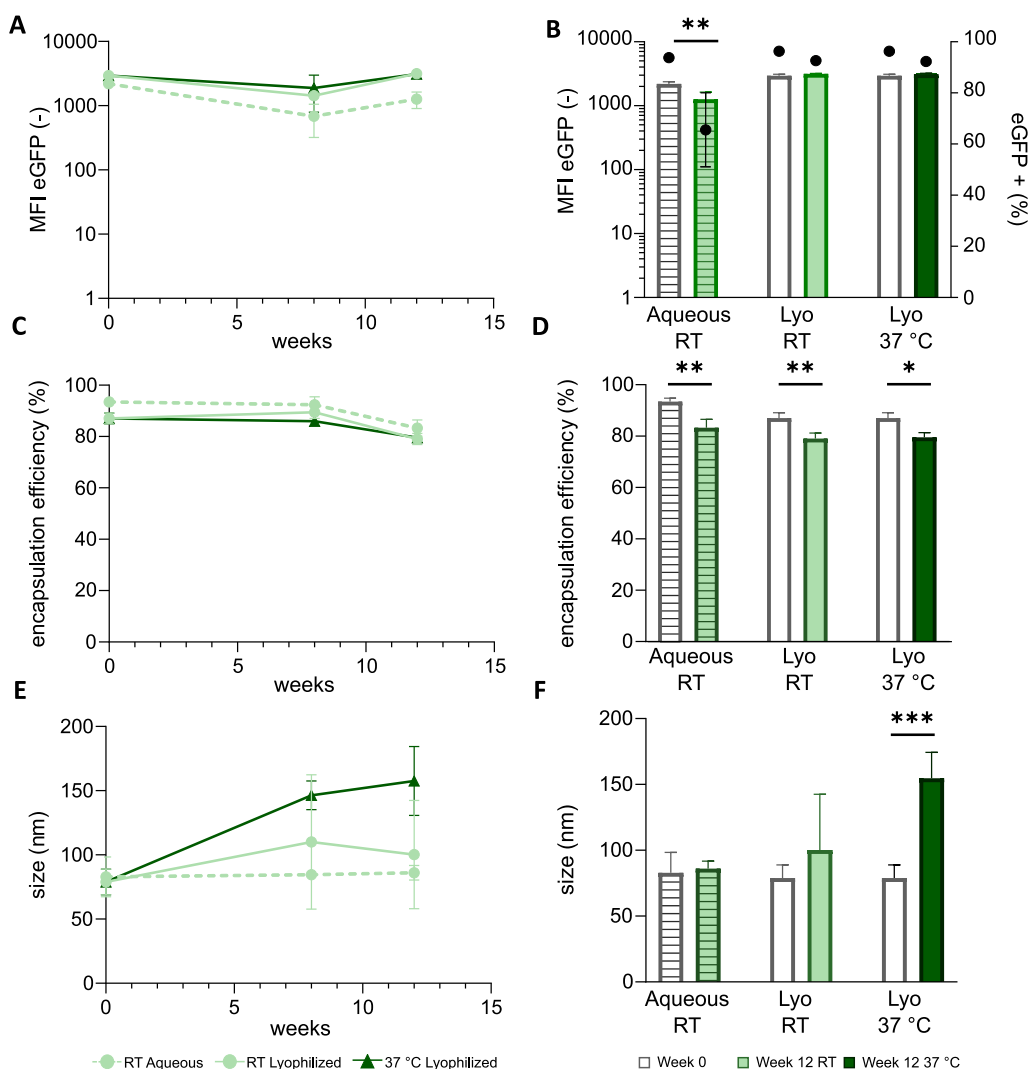


Fig. 5. Stability of aqueous and lyophilized mRNA LNPs at RT and 37 °C. eGFP encoding mRNA LNPs were formulated at a C12–200:mRNA wt ratio of 20 and subsequently dialyzed in Tris 20 mM with a pH of 7.4. mRNA LNPs were either stored in aqueous condition (dashed lines and bars) or in lyophilized condition in presence of 12.5 m/V% sucrose (full line) at 22 °C and 37 °C. (A, B) Transfection efficiency in HEK293T cells expressed as MFI eGFP in viable cells shown as a function of time (A) and at w0 (grey) and w12 (color) only (B). (C, D) Encapsulation efficiency determined via RiboGreen assay shown as a function of time (C) and at w0 and w12 only (D). (E, F) Size determined via DLS shown as a function of time (E) and at w0 and w12 only (F). Mean values are shown. Error bars represent geometric SD ($n = 3$ vials). One-way ANOVA was performed using Holm-Sidak correction. * $p < 0.05$, ** $p < 0.01$, *** $p < 0.001$.

ratio of 20 were suspended in Tris 20 mM containing 12.5 m/V% sucrose and were subsequently lyophilized and administered to mice at a dose of 3 μ g fLuc mRNA. As a positive control, an identical volumetric dose of freshly prepared fLuc mRNA LNPs was administered. Five hours after injection, in vivo protein expression was measured by bioluminescence imaging. In addition, in vitro transfection efficiency in HEK293T cells was measured before and after lyophilization by a luciferase assay, this to validate our freeze-drying protocol for mRNA LNPs formulated with another mRNA (i.e. fLuc) construct. Note that fLuc mRNA is longer than the eGFP mRNA construct used in the previous experiments.

As shown in Fig. 6A, the in vitro transfection efficiency of fLuc mRNA LNPs was similar before and after lyophilization, demonstrating that lyophilization can be applied to LNPs encapsulating various types of mRNA. This is an attractive observation as it is known that the length of the mRNA strand that is encapsulated might alter the properties of the mRNA LNPs [42]. Furthermore, in the mouse model, fLuc mRNA LNPs maintained mRNA expression efficiency after lyophilization (Fig. 6B-D).

4. Discussion

In this study we report on continuous freeze-drying of mRNA LNPs composed of the ionizable lipidoid C12–200 and evaluated the stability of the LNPs in various conditions. Freeze-drying comprises a freezing phase, a drying phase and reconstitution, which are all known to induce stresses to liposomal and lipid nanoparticle formulations [18–20]. As a

consequence, alterations of the CQAs of the product can occur. Lyoprotectants are typically used to avoid these stresses; indeed, their effectiveness has been demonstrated for lyophilization of RNA LNPs [21,23] and lipoplexes [43,44]. In most cases, saccharides such as sucrose and trehalose were used as lyoprotectants. Additionally, currently authorized mRNA vaccines also contain sucrose as a cryoprotectant to allow frozen storage [6,8]. Here, we used sucrose as lyoprotectant in a concentration of 12.5 m/V%. Whereas the importance of using the correct lyoprotectant has been reported multiple times, other factors that possibly affect stresses during lyophilization of LNPs have not yet been discussed.

We studied the effect of the ionizable lipid:mRNA wt ratio and the type of buffer on the physicochemical characteristics and transfection properties of mRNA LNPs following lyophilization. We observed that the encapsulation efficiency and zeta potential decreased significantly when mRNA LNPs with a low amount of lipids (i.e. a low C12–200:mRNA wt ratio) or suspended in a salt-containing buffer (PBS) were lyophilized. To understand why mRNA LNPs dialyzed in different buffers respond differently to lyophilization, we evaluated their morphology via cryo-EM and observed that mRNA LNPs showed a higher frequency of blebbed morphology upon dialysis in PBS compared to Tris. In fact, mRNA LNPs dialyzed in PBS even contained liposomal structures, most likely originating from dissociated blebs [40,45]. We hypothesize that this morphology could be correlated to the increased sensitivity toward the stresses occurring during lyophilization. Although mRNA LNPs show

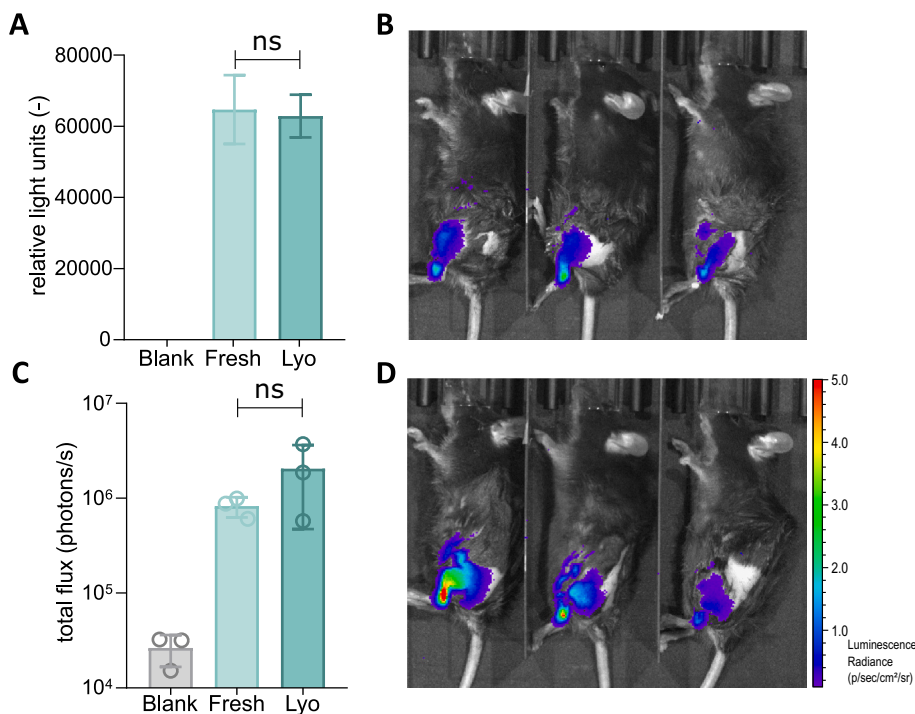


Fig. 6. Transfection efficiency of mRNA LNPs in vivo is maintained after freeze-drying. Firefly luciferase (fLuc) encoding mRNA LNPs were lyophilized in Tris 20 mM buffer with 12.5% sucrose as lyoprotectant. C57BL/6 mice were i.m. injected with fresh and lyophilized mRNA LNPs at a dose corresponding with 3 μ g luciferase mRNA, bioluminescence imaging was performed 5 h later. (A) In vitro HEK293T transfection efficiency determined via luciferase assay. (C) Total flux at ROI of the administration site determined via bioluminescence imaging. Mean values shown. Error bars represent standard deviation ($n = 3$). Unpaired t -test was performed ns = not significant. (B, D) Bioluminescence images of mice injected with fresh (B) and lyophilized fLuc LNPs (D).

important morphological differences in comparison with liposomes (LNPs typically consist of an amorphous lipid core whereas liposomes have an aqueous core) [46], there are some similarities that can potentially be employed to explain the observations mentioned above. Evidently, both nanoparticles are lipid-based and rely on lipid interactions but, more interestingly, the blebs that were observed in LNPs sensitive to lyophilization show remarkable similarities with liposomes [45]. As leakage of encapsulated drugs and RNA upon freeze-drying of liposomal formulations has frequently been reported in the past, it is possible that exactly this similarity with liposomes could explain the phenomena that were observed in this study [19]. In most cases, this leakage was attributed to fusion/aggregation processes and phase transitions taking place during freeze-drying [47]. When the temperature reaches the phase transition temperature (T_m), the permeability of liposomes becomes higher, resulting in leakage of the liposomal cargo. T_m is formulation-dependent and is typically higher in a dehydrated or lyophilized state, although this effect can be diminished by the use of lyoprotectants [48]. Nevertheless, several authors reported leakage of small molecules [49] and nucleic acids [50] despite using carbohydrate lyoprotectants. Guimarães et al. noted that leakage of hydrophilic drugs (methotrexate and doxorubicin) from DOPE/CH/DSPE-mPEG-liposomes could not be prevented, despite the use of lyoprotectants and optimizing several parameters [49]. Surprisingly, they did not detect drug leakage when a hydrophobic drug (tamoxifen) was encapsulated and concluded that drug leakage was dependent on the location of the drug in liposomes. Here, a similar effect on mRNA encapsulation efficiency was observed through lyophilization, despite the use of lyoprotectants (sucrose and trehalose).

Therefore, we hypothesize that also in our experiments the extent of (ionic) intermolecular interactions of mRNA with the lipids could prevent leakage during freeze-drying, explaining the advantage of using a formulation buffer with a low salt concentration (cf. PBS buffer vs. phosphate buffer), as salts can shield the charges on the ionizable lipids and as such diminish the ionic interactions between RNA and the ionizable lipid. From this perspective, it is important to mention the study of Okuda and colleagues who observed a diminished encapsulation efficiency after dialysis of mRNA LNPs in a buffer containing increasing concentrations of NaCl⁵¹. Here, we did not observe a

pronounced decrease in encapsulation efficiency after dialysis in PBS, but the weaker intermolecular interactions could clearly have contributed to the formation of blebs and consequent mRNA release during freeze-drying. Of note, Okuda et al. reported that this effect was dependent on the ionizable lipid and the helper lipid present in the formulation [51] which could explain why some studies report on the feasibility of lyophilization of RNA LNPs dispersed in PBS [21,23]. In addition, they also observed that the encapsulation efficiency of mRNA LNPs did not change in response to increasing salt concentrations in case of DOPE-inclusion but did change in case of DSPC/DOPC-inclusion [51]. Interestingly, in another study, it was found that blebs did not occur when DSPC was replaced by DOPE [39]. This, in combination with our cryo-EM of LNPs dialyzed in PBS, argues for the decisive role of salts in the formation of blebs. Moreover, the protective effect of the higher lipid:mRNA wt ratio also aligns with this hypothesis, as the increased presence of ionizable lipids could retain mRNA encapsulated in the ionizable lipid-rich amorphous core of the LNPs [39], avoiding bleb-formation. Interestingly, analogous to the effect of salts in the dialysis buffer, it was previously reported that formulations with a higher N:P ratio (N referring to the positive charges on the lipids, P referring to the negative charges on the nucleic acids) have an improved encapsulation efficiency, suggesting a beneficial effect of relatively more lipids on the interaction with mRNA [52].

Cryo-EM also revealed that lyophilization of PBS-dialyzed mRNA LNPs induced a phase transition from amorphous LNPs toward multilamellar LNPs. It has been reported that phase transitions can be induced by temperature- and pH shifts [53–56]. It should be noted that pH shifts may take place during freezing, especially when using a phosphate-based buffer for which a drop in pH of more than 3 units has been observed. Interestingly, Kulkarni et al. reported that siRNA LNPs contained siRNA sandwiched within lipid monolayers at pH 4, which converted into amorphous core LNPs at pH 7.4³⁸. Similar multilamellar structures as observed in our study were to date only reported for siRNA LNPs with N:P 1 [38]. Additionally, LNPs showing a certain degree of multilamellarity were observed when cholesterol was replaced with a derivate containing methyl and ethyl groups [56]. Multilamellar vesicles were also frequently reported for liposomal formulations [57,58]. However, given the limited number of publications reporting this

structure for RNA LNPs, it remains speculative what these LNPs represent and how lyophilization leads to the emergence of this morphology.

In the event that an optimal LNP composition (C12–200:mRNA wt ratio of 20:1) and optimal excipients (Tris or phosphate with 12.5 m/V% sucrose) were used, we showed that mRNA LNP characteristics and, most importantly, transfection efficiency were conserved. Note that we evaluated freeze-drying of C12–200-based mRNA LNPs with a composition similar to the marketed mRNA COVID vaccines. Nevertheless, optimal conditions for freeze-drying could be different when another lipid formulation is used. In this light, it is important to stress that C12–200 shows several structural differences compared to the ionizable lipids present in the marketed mRNA vaccines. More specifically, in contrast to ALC-0315 or SM-102, C12–200 contains multiple tertiary amines, of which two are in a piperazine group, and a branched structure with five alkyl groups, each of them containing one hydroxyl group. On the other hand, C12–200 does not contain ester groups in its lipid tail [59]. Next, the type of helper lipids and their molar ratio could strongly influence the stability of mRNA LNPs. As mentioned previously, phospholipids play an important role in the formation of blebs. Additionally, both cholesterol and phospholipids affect the T_m of lipid-based nanoparticles [46]. Therefore, the lipid composition could affect the stability of RNA LNPs during lyophilization as temperature changes are inherent to this process, and reaching the T_m is associated with (undesired) phase transitions [19]. Future work could focus on the role of helper lipids on mRNA LNP stability.

Also, employing other freeze-drying methods (e.g. classical batch freeze-drying) might impact the outcome. As mentioned previously, the continuous freeze-drying technology employed here starts with a spin-freezing step. Here, a vial containing the LNP formulation is spun along its longitudinal axis at high speeds, resulting in a layer of liquid on the walls of the glass vial. The liquid contents are subsequently solidified by the application of cooling gas, resulting in a layer of frozen material on the inner vial walls. Of note, previous research has demonstrated that the minor shear stresses generated during the ramp-up of the spin-freezing step are unlikely to be deleterious. Moreover, other process steps applied during the manufacturing, such as filtration and filling operations, induce much higher shear stresses than the spinning step [60].

Although the mechanisms underlying the instability of mRNA LNPs upon storage are largely unknown, hydrolysis of mRNA has been proposed as one of the key factors leading to the degradation of mRNA LNPs [61]. Therefore, lyophilization could be an ideal strategy to improve the long-term stability of mRNA LNP formulations. To evaluate this, we studied the stability of mRNA LNPs in aqueous or lyophilized form using Tris or phosphate buffer at 4 °C. At this temperature, we found that mRNA LNPs maintained their functionality for a period of 12 weeks both in aqueous and lyophilized conditions, which is similar to the prescribed shelf-life of 10 weeks for the pediatric and bivalent formulation of BNT162b2 [10,11]. Furthermore, it was also apparent that Tris buffer was superior to phosphate as the transfection efficiency decreased after only 1 week of storage of lyophilized mRNA LNPs in phosphate buffer. A recent report postulated a novel mechanism of instability of mRNA LNPs as it was found that oxidation and subsequent hydrolysis of the tertiary amine present in ionizable lipids generates aldehydes and secondary amines which can interact with mRNA to form lipid:mRNA adducts, rendering the encapsulated mRNA untranslatable [62]. Interestingly, Moderna recently reported that Tris acts as an aldehyde scavenger and as such promotes stability of mRNA LNPs [59,63]. However, it remains to be elucidated which mechanism could explain the difference between both buffers in our study.

We also performed a stability study at higher temperatures (RT and 37 °C) which demonstrated the added value of our lyophilization method for the storage of mRNA LNPs. Indeed, lyophilized LNPs retained their transfection efficiency when stored at RT or 37 °C; in contrast, for aqueous mRNA LNPs the transfection efficiency was drastically reduced after 12 weeks of storage. Although stability at higher

temperatures is necessary to avoid cold chain logistics, there are currently no reports available which show that mRNA LNPs survive a period of 12 weeks at 22 °C or higher. For LNPs stored at RT some studies only showed stability over a limited period (1 week [64] to 4 weeks [24]) while other studies observed a decreased fLuc expression after 4 weeks [25] or EPO-expression after 4 weeks [65]. Furthermore, mRNA expression was diminished upon storage at 37–42 °C in all of the aforementioned studies. We thus believe that our lyophilization method represents a promising step forward to improve the stability of mRNA vaccines for storage at higher temperatures.

Some changes were observed in the physicochemical characteristics of lyophilized mRNA LNPs stored at 37 °C. The LNPs increased in size when stored for longer periods at high temperatures (37 °C), while no size differences were observed at RT storage. This agrees with earlier observations on lyophilization of mRNA LNPs [25]. Since LNPs used in this study have a PEG shell, it is less likely that the LNPs have aggregated during the stability study. More probably, particles grew as a consequence of the Ostwald-ripening effect, as already described for siRNA LNPs based on low molecular weight ionizable lipids [66]. We also noted that when mRNA LNPs were stored at RT and 37 °C, a slight decrease in encapsulation efficiency for both lyophilized mRNA LNPs and aqueous mRNA LNPs occurred. Nevertheless, the encapsulation efficiency was stable for a period of 8 weeks in both cases.

In conclusion, we present a method to lyophilize mRNA LNPs based on the ionizable lipidoid C12–200 using a continuous freeze-drying technology based on spin freezing. We showed that, when the lipid:mRNA weight ratio was sufficiently high and Tris or phosphate, but not PBS, was used as a buffer, the properties of the mRNA LNPs were unchanged after freeze-drying. Cryo-EM images revealed important insight into the buffer-dependent behavior of LNPs during formation and lyophilization. In addition, we showed that lyophilization of fLuc mRNA LNPs did not change *in vivo* luciferase expression in mice. We demonstrated that lyophilization of mRNA LNPs is an attractive strategy to enhance the stability of mRNA vaccines at higher temperatures, as lyophilized mRNA LNPs preserved their functionality when stored at 4 °C, 22 °C and even at 37 °C for a period of 12 weeks. To our knowledge, this is the first study that demonstrates that lyophilization enhances the stability of mRNA LNPs allowing their storage at higher temperatures for a prolonged period.

CRediT authorship contribution statement

Sofie Meulewaeter: Investigation, Formal analysis, Writing – original draft. **Gust Nuytten:** Investigation, Writing – original draft, Methodology. **Miffy H.Y. Cheng:** Investigation, Formal analysis, Methodology. **Stefaan C. De Smedt:** Writing – review & editing. **Pieter R. Cullis:** Methodology. **Thomas De Beer:** Writing – review & editing, Methodology. **Ine Lentacker:** Writing – review & editing, Conceptualization. **Rein Verbeke:** Investigation, Writing – review & editing, Conceptualization.

Declaration of Competing Interest

R.V., I.L., and S.D.S. are contributors to patent applications no. WO2020058239A1; Therapeutic nanoparticles and methods of use thereof, and no. EP22170845.6; Vaccine Compositions against *Listeria* Infection.

Data availability

Data will be made available on request.

Acknowledgements

We thank the UBC High Resolution Macromolecular Cryo-Electron Microscopy Facility (HRMEM) for their support with the cryo-EM

imaging. S.M. is a doctoral fellow from the Research Foundation-Flanders (FWO-V) (grant number 1S73120N). R.V. is a postdoctoral fellow from the Research Foundation-Flanders (FWO-V) (grant number 1275023N) and acknowledges the FWO-V travel grant V407822N. M.H. Y.C. is funded by NMIN postdoctoral fellowship in gene therapy. This work was supported by a grant of Kom Op Tegen Kanker (Stand up to Cancer, grant number KotK_UGent/2018/11466/1). I.L. would like to acknowledge funding from Ghent University Concerted Research Action (grant number BOF21/GOA/033). I.L. and S.D.S. would like to acknowledge funding from Research Foundation Flanders (FWO-V) (grant number G040319N). R.V. would like to acknowledge funding from King Baudouin Foundation (grant number 2020-J1811380-217916). I.L. and S.D.S. acknowledge support from European Union's Horizon Europe research and innovation program under grant agreement No 101080544 (Baxerna2.0).

Appendix A. Supplementary data

Supplementary data to this article can be found online at <https://doi.org/10.1016/j.jconrel.2023.03.039>.

References

- R. Verbeke, I. Lentacker, S.C. de Smedt, H. Dewitte, The dawn of mRNA vaccines: the COVID-19 case, *J. Control. Release* 333 (2021) 511–520, <https://doi.org/10.1016/j.jconrel.2021.03.043>.
- EMA, European Medicines Agency. Comirnaty, Comirnaty Original/Omicron BA.1, Comirnaty Original/Omicron BA.4–5 (COVID-19 mRNA Vaccine) Risk Management Plan, Accessed November 15, 2022, from, https://www.ema.europa.eu/en/documents/rmp-summary/comirnaty-epar-risk-management-plan_en.pdf, 2022, September.
- EMA, European Medicines Agency. Comirnaty, Comirnaty Original/Omicron BA.1, Comirnaty Original/Omicron BA.4–5 (COVID-19 mRNA Vaccine) Risk Management Plan, Accessed November 15, 2022, from, https://www.ema.europa.eu/en/documents/rmp-summary/comirnaty-epar-risk-management-plan_en.pdf, 2022, September.
- M.N. Uddin, M.A. Roni, Challenges of storage and stability of mRNA-based COVID-19 vaccines, *Vaccines* 9 (9) (2021) 1033, <https://doi.org/10.3390/VACCINES9091033>.
- D.J.A. Crommelin, T.J. Anchordoquy, D.B. Volkin, W. Jiskoot, E. Mastrobattista, Addressing the cold reality of mRNA vaccine stability, *J. Pharm. Sci.* 110 (3) (2021) 997–1001, <https://doi.org/10.1016/j.xphs.2020.12.006>.
- EMA. *Spikevax (previously covid-19 vaccine moderna)*, *Product Information*, European Medicines Agency, 2021. Available at, https://www.ema.europa.eu/en/documents/product-information/spikevax-previously-covid-19-vaccine-moderna-epar-product-information_en.pdf (Accessed: November 15, 2022).
- EMA, European Medicines Agency. Assessment report COVID-19 Vaccine Moderna, Accessed November 15, 2022, from, https://www.ema.europa.eu/en/documents/assessment-report/spikevax-previously-covid-19-vaccine-moderna-epar-public-assessment-report_en.pdf, 2021, March 11.
- Comirnaty 30 micrograms/dose concentrate for dispersion for injection 12+ years COVID-19 mRNA Vaccine (nucleoside modified) - Summary of Product Characteristics (SmPC) - (emc), Accessed July 23, 2022, https://www.medicines.org.uk/emc/product/12740/smpc#SHELF_LIFE.
- CHMP, Committee for Medicinal Products for Human Use (CHMP) CHMP Assessment Report on Group of An Extension of Marketing Authorisation and Variations, Accessed October 25, 2022, www.ema.europa.eu/contact, 2021.
- Comirnaty Original/Omicron BA.1 15/15 micrograms per dose dispersion for injection COVID-19 mRNA Vaccine (nucleoside modified) - Summary of Product Characteristics (SmPC) - (emc), Accessed November 3, 2022, https://www.medicines.org.uk/emc/product/13134/smpc#SHELF_LIFE.
- Comirnaty 10 micrograms/dose concentrate for dispersion for injection Children 5 to 11 years COVID-19 mRNA Vaccine (nucleoside modified) - Summary of Product Characteristics (SmPC) - (emc), Accessed July 23, 2022, https://www.medicines.org.uk/emc/product/13134/smpc#SHELF_LIFE.
- EMA. (n.d.). Annex I Summary of Product Characteristics - European Medicines Agency. Annex I Summary of Product Characteristics. Accessed November 15, 2022, from https://www.ema.europa.eu/en/documents/product-information/vaxzevria-previously-covid-19-vaccine-astrazeneca-epar-product-information_en.pdf.
- EMA. (n.d.). Annex I Summary of Product Characteristics - European Medicines Agency. Annex I Summary of Product Characteristics. Retrieved November 15, 2022, from https://www.ema.europa.eu/en/documents/product-information/nuvaxovid-epar-product-information_en.pdf.
- EMA. (n.d.). Jcovden (previously COVID-19 Vaccine Janssen). European Medicines Agency. Accessed November 15, 2022, from <https://www.ema.europa.eu/en/medicines/human/EPAR/jcovden-previously-covid-19-vaccine-janssen>.
- D. Feyisa, F. Ejeta, T. Aferu, O. Kebede, Adherence to WHO vaccine storage codes and vaccine cold chain management practices at primary healthcare facilities in Dalocha District of Silt'e zone, Ethiopia, *Trop. Dis. Travel. Med. Vaccines* 8 (1) (2022), <https://doi.org/10.1186/S40794-022-00167-5>.
- M.L. Fahrni, I.A.N. Ismail, D.M. Refi, et al., Management of COVID-19 vaccines cold chain logistics: a scoping review, *J. Pharm. Policy Pract.* 15 (1) (2022) 1–14, <https://doi.org/10.1186/S40545-022-00411-5/TABLES/1>.
- Z. Ghaemmaghamian, R. Zarghami, G. Walker, E. O'Reilly, A. Ziaee, Stabilizing vaccines via drying: quality by design considerations, *Adv. Drug Deliv. Rev.* 187 (2022), 114313, <https://doi.org/10.1016/J.ADDR.2022.114313>.
- C. Chen, D. Han, C. Cai, X. Tang, An overview of liposome lyophilization and its future potential, *J. Control. Release* 142 (3) (2010) 299–311, <https://doi.org/10.1016/J.JCONREL.2009.10.024>.
- E. Trenkenschuh, W. Friess, Freeze-drying of nanoparticles: how to overcome colloidal instability by formulation and process optimization, *Eur. J. Pharm. Biopharm.* 165 (2021) 345–360, <https://doi.org/10.1016/J.EJPB.2021.05.024>.
- S. Franzé, F. Selmin, E. Samaritani, P. Minghetti, F. Ciliruzo, Lyophilization of liposomal formulations: still challenging, *Pharmaceutics* 10 (3) (2018), <https://doi.org/10.3390/PHARMACEUTICS10030139>.
- P. Zhao, X. Hou, J. Yan, et al., Long-term storage of lipid-like nanoparticles for mRNA delivery, *Bioact. Mater.* 5 (2) (2020) 358, <https://doi.org/10.1016/J.BIOACTMAT.2020.03.001>.
- B. Kim, R.R. Hosn, T. Remba, et al., Optimization of storage conditions for lipid nanoparticle-formulated self-replicating RNA vaccines, *J. Control. Release* 353 (2023) 241–253, <https://doi.org/10.1016/j.jconrel.2022.11.022>.
- Ball Rebecca, P. Bajaj, K. Whitehead, Achieving long-term stability of lipid nanoparticles: examining the effect of ph, temperature, and lyophilization, *Int. J. Nanomedicine* 12 (2017) 305, <https://doi.org/10.2147/IJN.S123062>.
- Y. Suzuki, T. Miyazaki, H. Muto, et al., Design and lyophilization of lipid nanoparticles for mRNA vaccine and its robust immune response in mice and nonhuman primates, *Mol. Ther. Nucleic Acids* 30 (2022) 226–240, <https://doi.org/10.1016/J.OMTN.2022.09.017>.
- H. Muramatsu, K. Lam, C. Bajusz, et al., Lyophilization provides long-term stability for a lipid nanoparticle-formulated, nucleoside-modified mRNA vaccine, *Mol. Ther.* 30 (5) (2022) 1941–1951, <https://doi.org/10.1016/J.YMTHE.2022.02.001>.
- L.C. Capozzi, B.L. Trout, R. Pisano, From batch to continuous: freeze-drying of suspended vials for Pharmaceuticals in Unit-Doses, *Ind. Eng. Chem. Res.* 58 (4) (2019) 1635–1649, https://doi.org/10.1021/ACS.IECR.8B02886/ASSET/IMAGES/LARGE/IE-2018-028869_0014.JPEG.
- X. Tang, M.J. Pikal, Design of freeze-drying processes for pharmaceuticals: practical advice, *Pharm. Res.* 21 (2) (2004) 191–200, <https://doi.org/10.1023/B:PHAM.0000016234.73023.75>.
- L. de Meyer, P.J. van Bockstal, J. Corver, C. Vervaet, J.P. Remon, T. de Beer, Evaluation of spin freezing versus conventional freezing as part of a continuous pharmaceutical freeze-drying concept for unit doses, *Int. J. Pharm.* 496 (1) (2015) 75–85, <https://doi.org/10.1016/J.IJPHARM.2015.05.025>.
- G. Allison, Y.T. Cain, C. Cooney, et al., Regulatory and quality considerations for continuous manufacturing may 20–21, 2014 continuous manufacturing symposium, *J. Pharm. Sci.* 104 (3) (2015) 803–812, <https://doi.org/10.1002/JPS.24324>.
- US10670336B2 - Method and system for freeze-drying injectable compositions, in particular pharmaceutical compositions - Google Patents, Accessed July 25, 2022, <https://patents.google.com/patent/US10670336B2/en>.
- L. Leys, B. Vanbillemont, P.J. van Bockstal, et al., A primary drying model-based comparison of conventional batch freeze-drying to continuous spin-freeze-drying for unit doses, *Eur. J. Pharm. Biopharm.* 157 (2020) 97–107, <https://doi.org/10.1016/J.EJPB.2020.09.009>.
- J. Lammens, N.M. Goudarzi, L. Leys, et al., Spin freezing and its impact on pore size, tortuosity and solid state, *Pharmaceutics* 13 (12) (2021), <https://doi.org/10.3390/PHARMACEUTICS13122126>.
- P.J. van Bockstal, L. de Meyer, J. Corver, C. Vervaet, T. de Beer, Noncontact infrared-mediated heat transfer during continuous freeze-drying of unit doses, *J. Pharm. Sci.* 106 (1) (2017) 71–82, <https://doi.org/10.1016/J.XPHS.2016.05.003>.
- G. Nuytten, S.R. Revatta, P.J. van Bockstal, et al., Development and application of a mechanistic cooling and freezing model of the spin freezing step within the framework of continuous freeze-drying, *Pharmaceutics* 13 (12) (2021) 2076, <https://doi.org/10.3390/PHARMACEUTICS13122076>.
- L. Leys, G. Nuytten, J. Lammens, et al., A NIR-based study of desorption kinetics during continuous spin freeze-drying, *Pharmaceutics* 13 (12) (2021), <https://doi.org/10.3390/PHARMACEUTICS13122168>.
- F. Leuschner, P. Dutta, R. Gorbato, et al., Therapeutic siRNA silencing in inflammatory monocytes, *Nat. Biotechnol.* 29 (11) (2011) 1005, <https://doi.org/10.1038/NBT.1989>.
- R. Verbeke, I. Lentacker, S.C. de Smedt, H. Dewitte, The dawn of mRNA vaccines: the COVID-19 case, *J. Control. Release* 333 (2021) 511–520, <https://doi.org/10.1016/J.JCONREL.2021.03.043>.
- J.A. Kulkarni, M.M. Darjuan, J.E. Mercer, et al., On the formation and morphology of lipid nanoparticles containing ionizable cationic lipids and siRNA, *ACS Nano* 12 (5) (2018) 4787–4795, https://doi.org/10.1021/ACS.NANO.8B01516/ASSET/IMAGES/LARGE/NN-2018-01516S_0006.JPEG.
- A.K.K. Leung, Y.Y.C. Tam, S. Chen, I.M. Hafez, P.R. Cullis, Microfluidic mixing: a general method for encapsulating macromolecules in lipid nanoparticle systems, *J. Phys. Chem. B* 119 (28) (2015) 8698–8706, <https://doi.org/10.1021/ACS.JPCB.5B02891>.
- M.L. Brader, S.J. Williams, J.M. Banks, W.H. Hui, Z. Hong Zhou, L. Jin, Encapsulation state of messenger RNA inside lipid nanoparticles, *Biophys. J.* 120 (2021) 2766–2770, <https://doi.org/10.1016/j.bpj.2021.03.012>.

- [41] Henderson MI, Eygeris Y, Jozic A, Herrera M, Sahay G. Leveraging biological buffers for efficient messenger RNA delivery via lipid nanoparticles. *Mol. Pharm.* 21, 2022. doi:<https://doi.org/10.1021/ACS.MOLPHARMACEUT.2C00587>.
- [42] J.A. Kulkarni, D. Witzigmann, J. Leung, Y.Y.C. Tam, P.R. Cullis, On the role of helper lipids in lipid nanoparticle formulations of siRNA, *Nanoscale*. 11 (45) (2019) 21733–21739, <https://doi.org/10.1039/C9NR09347H>.
- [43] P. Yadava, M. Gibbs, C. Castro, J.A. Hughes, Effect of lyophilization and freeze-thawing on the stability of siRNA-liposome complexes, *AAPS PharmSciTech* 9 (2) (2008) 335–341, <https://doi.org/10.1208/S12249-007-9000-1/FIGURES/6>.
- [44] M. Tang, S. Hu, Y. Hattori, Effect of pre-freezing and saccharide types in freeze-drying of siRNA lipoplexes on gene-silencing effects in the cells by reverse transfection, *Mol. Med. Rep.* 22 (4) (2020) 3233–3244, <https://doi.org/10.3892/MMR.2020.11419/HTML>.
- [45] M. Kloczewiak, J.M. Banks, L. Jin, M.L. Brader, A biopharmaceutical perspective on higher-order structure and thermal stability of mRNA vaccines, *Mol. Pharm.* (July 4, 2022), <https://doi.org/10.1021/ACS.MOLPHARMACEUT.2C00092>.
- [46] C. Hald Albertsen, J.A. Kulkarni, D. Witzigmann, M. Lind, K. Petersson, J. B. Simonsen, The role of lipid components in lipid nanoparticles for vaccines and gene therapy, *Adv. Drug Deliv. Rev.* 188 (2022), 114416, <https://doi.org/10.1016/J.ADDR.2022.114416>.
- [47] R.W. Nugraheni, N.A. Mulyadi, H. Yusuf, Freeze-dried liposome formulation for small molecules, nucleic acid, and protein delivery, *System. Rev. Pharm.* 11 (7) (2020) 143–151, <https://doi.org/10.31838/SRP.2020.7.23>.
- [48] K.L. Koster, M.S. Webb, G. Bryant, D. Lynch, v., Interactions between soluble sugars and POPS (1-palmitoyl-2-oleoylphosphatidylcholine) during dehydration: vitrification of sugars alters the phase behavior of the phospholipid, *Biochim. Biophys. Acta* 1193 (1) (1994) 143–150, [https://doi.org/10.1016/0005-2736\(94\)90343-3](https://doi.org/10.1016/0005-2736(94)90343-3).
- [49] D. Guimarães, J. Noro, C. Silva, A. Cavaco-Paulo, E. Nogueira, Protective effect of saccharides on freeze-dried liposomes encapsulating drugs, *Front. Bioeng. Biotechnol.* 7 (2019) 424, <https://doi.org/10.3389/FBIOE.2019.00424/BIBTEX>.
- [50] H. Lee, D. Jiang, W.M. Pardridge, Lyoprotectant optimization for the freeze-drying of receptor-targeted Trojan horse liposomes for plasmid DNA delivery, *Mol. Pharm.* 17 (6) (2020) 2165–2174, https://doi.org/10.1021/ACS.MOLPHARMACEUT.0C00310/ASSET/IMAGES/LARGE/MP0C00310_0006.JPEG.
- [51] K. Okuda, Y. Sato, K. Iwakawa, et al., On the size-regulation of RNA-loaded lipid nanoparticles synthesized by microfluidic device, *J. Control. Release* 348 (2022) 648–659, <https://doi.org/10.1016/J.JCONREL.2022.06.017>.
- [52] M.J. Carrasco, S. Alishetty, M.G. Alameh, et al., Ionization and structural properties of mRNA lipid nanoparticles influence expression in intramuscular and intravascular administration, *Commun. Biol.* 4 (1) (2021) 1–15, <https://doi.org/10.1038/s42003-021-02441-2>.
- [53] N.R. Larson, G. Hu, Y. Wei, A.D. Tieska, M.L. Forrest, C.R. Middaugh, pH-dependent phase behavior and stability of cationic lipid–mRNA nanoparticles, *J. Pharm. Sci.* 111 (3) (2022) 690–698, <https://doi.org/10.1016/J.XPHS.2021.11.004>.
- [54] M.Y. Arteta, T. Kjellman, S. Bartesaghi, et al., Successful reprogramming of cellular protein production through mRNA delivered by functionalized lipid nanoparticles, *Proc. Natl. Acad. Sci. U. S. A.* 115 (15) (2018) E3351–E3360, https://doi.org/10.1073/PNAS.1720542115/SUPPL_FILE/PNAS.201720542SI.PDF.
- [55] L. Uebbing, A. Ziller, C. Siewert, et al., Investigation of pH-responsiveness inside lipid nanoparticles for parenteral mRNA application using small-angle X-ray scattering, *Langmuir*. 36 (44) (2020) 13331–13341, https://doi.org/10.1021/ACS.LANGMUIR.0C02446/ASSET/IMAGES/MEDIUM/LA0C02446_M005.GIF.
- [56] Y. Eygeris, S. Patel, A. Jozic, G. Sahay, G. Sahay, Deconvoluting lipid nanoparticle structure for messenger RNA delivery, *Nano Lett.* 20 (6) (2020) 4543–4549, https://doi.org/10.1021/ACS.NANOLETT.0C01386/ASSET/IMAGES/LARGE/NL0C01386_0005.JPEG.
- [57] S.R. Bandara, T.G. Molley, H. Kim, P.A. Bharath, K.A. Kilian, C. Leal, The structural fate of lipid nanoparticles in the extracellular matrix, *Mater. Horiz.* 7 (1) (2020) 125, <https://doi.org/10.1039/C9MH00835G>.
- [58] S. Weisman, D. Hirsch-Lerner, Y. Barenholz, Y. Talmon, Nanostructure of cationic lipid-oligonucleotide complexes, *Biophys. J.* 87 (1) (2004) 609–614, <https://doi.org/10.1529/BIOPHYSJ.103.033480>.
- [59] E.O. Blenke, E. Ørnsmov, C. Schöneich, et al., The storage and in-use stability of mRNA vaccines and therapeutics: not a cold case, *J. Pharm. Sci.* (November 2022), <https://doi.org/10.1016/J.XPHS.2022.11.001>.
- [60] J. Lammens, S.T.F.C. Mortier, L. de Meyer, et al., The relevance of shear, sedimentation and diffusion during spin freezing, as potential first step of a continuous freeze-drying process for unit doses, *Int. J. Pharm.* 539 (1–2) (2018) 1–10, <https://doi.org/10.1016/J.IJPHARM.2018.01.009>.
- [61] L. Schoenmaker, D. Witzigmann, J.A. Kulkarni, et al., mRNA-lipid nanoparticle COVID-19 vaccines: structure and stability, *Int. J. Pharm.* 601 (2021), 120586, <https://doi.org/10.1016/J.IJPHARM.2021.120586>.
- [62] M. Packer, D. Gyawali, R. Yerabolu, J. Schariter, P. White, A novel mechanism for the loss of mRNA activity in lipid nanoparticle delivery systems, *Nat. Commun.* 12 (1) (2021) 1–11, <https://doi.org/10.1038/s41467-021-26926-0>.
- [63] P. White, Moderna Science and Technology Day, 2023.
- [64] N.N. Zhang, X.F. Li, Y.Q. Deng, et al., A thermostable mRNA vaccine against COVID-19, *Cell*. 182 (5) (2020) 1271–1283.e16, <https://doi.org/10.1016/J.CELL.2020.07.024>.
- [65] M. Ripoll, M.C. Bernard, C. Vaure, et al., An imidazole modified lipid confers enhanced mRNA-LNP stability and strong immunization properties in mice and non-human primates, *Biomaterials*. 286 (2022), 121570, <https://doi.org/10.1016/J.BIOMATERIALS.2022.121570>.
- [66] M.E. Gindy, B. Feuston, A. Glass, et al., Stabilization of oswald ripening in low molecular weight amino lipid nanoparticles for systemic delivery of siRNA therapeutics, *Mol. Pharm.* 11 (11) (2014) 4143–4153, https://doi.org/10.1021/MP500367K/SUPPL_FILE/MP500367K_SI_001.PDF.